Direct shape control of photoreduced nanostructures on proton exchanged ferroelectric templates

Laila Balobaid,[1] N. Craig Carville,[1,2] Michele Manzo,[3] Katia Gallo,[3] and Brian J. Rodriguez[1,2,a)]
[1]*School of Physics, University College Dublin, Belfield, Dublin 4, Ireland*
[2]*Conway Institute of Biomolecular and Biomedical Research, University College Dublin, Belfield, Dublin 4, Ireland*
[3]*Department of Applied Physics, KTH - Royal Institute of Technology, Roslagstullbacken 21, 106 91 Stockholm, Sweden*

(Received 15 November 2012; accepted 10 January 2013; published online 31 January 2013)

Photoreduction on a periodically proton exchanged ferroelectric crystal leads to the formation of periodic metallic nanostructures on the surface. By varying the depth of the proton exchange (PE) from 0.59 to 3.10 μm in congruent lithium niobate crystals, the width of the lateral diffusion region formed by protons diffusing under the mask layer can be controlled. The resulting deposition occurs in the PE region with the shallowest PE depth and preferentially in the lateral diffusion region for greater PE depths. PE depth-control provides a route for the fabrication of complex metallic nanostructures with controlled dimensions on chemically patterned ferroelectric templates. © *2013 American Institute of Physics*. [http://dx.doi.org/10.1063/1.4789412]

The controlled deposition of metallic nanostructures onto substrates has promising potential for biosensing[1] and surface enhanced Raman scattering applications.[2–4] One route is the photoreduction on ferroelectric surfaces by illuminating a sample immersed in aqueous $AgNO_3$ with super-bandgap energy light. This leads to the reduction of Ag^+ to Ag^0 where the electrons accumulate, allowing for the fabrication of silver nanostructures on specified regions, i.e., positive or negative domains, and along domain walls or chemically patterned interfaces, depending on the deposition conditions and the sample properties.[5–16] Congruent lithium niobate (LN) is one of the most studied ferroelectric crystals due to its large electro-optic and electro-mechanical coupling coefficients and has been used extensively for photodeposition studies.[4,5,11–13,16]

Illuminating LN with UV light of energies higher than the bandgap ($E_g \sim 3.9$ eV, which corresponds to a wavelength of $\lambda < 318$ nm)[17] allows the photogeneration of electron-hole pairs that can participate in reduction and oxidation reactions.[10] When photochemical reactions have been employed to fabricate silver nanowires on a domain patterned ferroelectric template, i.e., periodically poled lithium niobate (PPLN), the nanostructures are confined to the 180° domain walls.[11,14] The location of the nanowires can be controlled by varying the domain pattern configurations, which requires electric field poling.[11] The dependence on other factors, including polarization screening, concentration, wavelength, temperature, and irradiation time, can influence whether the deposition takes place on the domain wall or on certain domains.[10,15,16] However, for the cases where nanowires form, the nanowires are always confined to the domain wall, i.e., the shape cannot be controlled.

Previously, we demonstrated that chemical patterning via proton exchange (PE) through a photolithographically defined mask[18,19] effectively modifies the electric fields at the surface of the LN crystal, which can then be used to fabricate metallic nanostructures.[4,5] PE is a chemical-based technique employed for the fabrication of optical waveguides in LN that allows the exchange of hydrogen ions from a proton source (benzoic acid) with lithium ions in the crystal (see Eq. (1)), which implies the degradation of both the ferroelectric and piezoelectric properties,[20]

$$LiNbO_3 + xH^+ \rightleftharpoons Li_{1-x}H_xNbO_3 + xLi^+. \quad (1)$$

Photodeposition on such surfaces causes silver nanostructures to form preferentially at the interface between the PE and LN regions, specifically in the region that forms during the PE process when protons diffuse under the Ti masking layer, i.e., the lateral diffusion region (LD).[4] The nanostructure formation is likely to depend on polarization screening, light intensity, and wavelength, although only the effect of $AgNO_3$ concentration has been studied in detail on periodic PE:LN (PPE:LN) surfaces.[5] There are several advantages of PE over electric field poling to form such nanostructures. First, the process avoids the technological complications of electric field poling, which typically involves the application of high fields (21 kV/mm) and several challenges in achieving controllable domain features due to domain broadening during poling. Second, nanowires formed on PPLN can only be as wide as the domain wall. Third, the structures must adhere to the geometry of the poled domains, which is restricted by crystallography. Here, we show that by calibrating the time-dependent depth of the PE region (d_{PE_z}), the width of the LD region is simultaneously adjusted, thereby allowing us to control the width of the formed nanostructures.

The PPE:LN samples were fabricated using a combination of photolithography and PE processes as described before.[4,18,19] Briefly, the photolithography on 500 μm thick z-cut congruent LN (Castech) included Ti evaporation and

a)Author to whom correspondence should be addressed. Electronic mail: brian.rodriguez@ucd.ie.

TABLE I. The measured PE depths in the different LN crystals.

Depth d_{PE_z} (μm)	t_{PE_z} (min)
0.59	52
1.21	210
1.79	480
2.30	852
2.72	1332
3.10	1920

reactive-ion etching (RIE) (12.17 μm period with ~50% duty cycle) on the –z surface, followed by a PE process realized by immersing the samples in pure benzoic acid (C_6H_5COOH) at 200 °C. The metallic mask was then etched in a dilute HF:H_20 solution for a few seconds. Optical characterizations with a prism coupler (Metricon, 2010/M) were employed to quantify the depth of the PE region.[21]

Prior to photodeposition, the samples were cleaned using sonication for 20 min each in acetone, isopropanol, and Milli-Q water (18.2 MΩ/cm), respectively. The silver deposition was carried out in 70 μl of a 0.01 M $AgNO_3$ solution (Sigma Aldrich) during illumination with a UV pen lamp of 254 nm wavelength and nominal 1400 μW/cm^2 power output (Spectroline) for 5 min at a fixed distance of 2 cm. Amplitude modulation atomic force microscopy (AM-AFM) (Asylum Research, MFP-3D) operated in repulsive mode and equipped with doped AFM tips (Nanosensors, PPP-NCH (resonant frequency, 332 kHz, spring constant, 42 N/m)) was used to probe the surfaces before and after each photodeposition experiment. The same cleaning procedure was used after deposition to remove the silver from the surface in order to reuse the samples; however, after acetone sonication, the sample was rubbed lightly with lens paper soaked in isopropanol.

To investigate the effect of varying the depth of the PE region in *z*-cut LN crystals, we have studied crystals that have been periodically proton exchanged for the times (t_{PE_z}) shown in Table I. The length of time that the crystal is exposed to the proton source determines the depth of the proton exchanged area,[22] as shown in Eq. (2)

$$d_{PE_z} = \sqrt{4\ D_{PE_z}(T_{PE})t_{PE_z}}\ , \tag{2}$$

where $D_{PE_z}(T_{PE})$ is the diffusion constant of hydrogen in $LiNbO_3$ in the *z*-direction at $T_{PE} = 200\,°C$.[22] The depths were profiled optically using a prism coupling technique, the results of which are also shown in Table I. The experimentally determined depths range from 0.59 to 3.10 μm, corresponding to a constant of diffusion in the *z*-direction of $0.084 \pm 0.004\ \mu m^2/h$.

Periodically proton-exchanging the LN substrate leads to the creation of an inhomogeneous electric field distribution at each PE:LN interface. Increasing the depth of the periodic PE layers results in the broadening of the LD region that is formed due to H^+ diffusion under the Ti mask.[14] The AFM topography images of three of the samples studied with different PE depths are shown in Figs. 1(a)–1(c). The sample with the shallowest d_{PEz} has the narrowest LD region, as determined from the topographic features associated with swelling. This swelling is a consequence of the strain associated with the inclusion of protons in the crystal lattice of LN.[23] A PE depth of 0.59 μm corresponds to a lateral diffusion width (W_{LD}) of 0.280 ± 0.045 μm (Fig. 1(a)), as determined from the mean and standard deviation of 10 line profiles (n = 10) measured perpendicular to the periodic pattern. The AFM topography of samples with $d_{PEz} = 1.21$ and 3.10 μm are shown in Figs. 1(b) and 1(c), from which W_{LD} has been determined to be 0.615 ± 0.054 μm

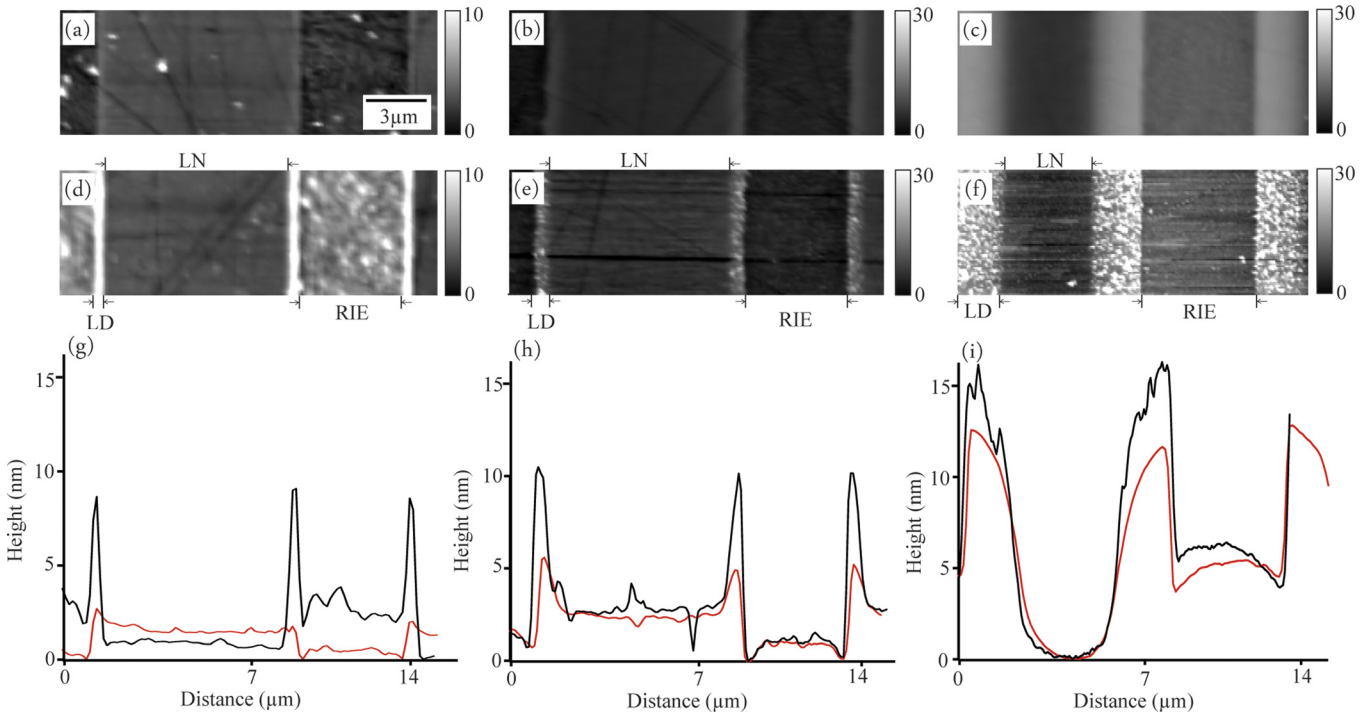

FIG. 1. AFM topography images of PPE:LN surfaces (a)–(c) before and (d)–(f) after Ag deposition for samples with PE depths of 0.59, 1.21, and 3.10 μm, respectively. (g)–(i) Graphs of the *y*-averaged images, showing the profile of the surfaces before (red) and after (black) Ag deposition.

and $2.190 \pm 0.081\ \mu$m, respectively (n = 10). Profiles of the *y*-averaged images (Figs. 1(a)–1(c)) are shown as red lines in Figs. 1(g)–1(i), respectively. In Figs. 1(a) and 1(g), it is clear that the RIE process (trench region) removes some LN material and also that there is very little swelling associated with PE for an exposure time of 52 min. For larger PE depths [Figs. 1(b), 1(c), 1(h), and 1(i)], it is clear that the PE regions exhibit more swelling and that they encroach on the pure LN regions. After exposure to UV light in solution, Ag nanostructures have formed on the surface of the PE region ($W_{RIE} + W_{LD}$) for $d_{PEz} = 0.59\ \mu$m (Fig. 1(d)), presumably under a predominant action of the normal component of the electric field embedded just underneath the crystal surface (at the shallow PE-LN interface). For $d_{PEz} \geq 1.21\ \mu$m, however, nanostructures have formed which are confined to the LD regions of each sample (see Figs. 1(e) and 1(f)). This behavior observed for the larger PE depths is attributed to the inhomogeneous tangential fields found at the PE:LN interfaces at the surface of the crystal and to the differences in bandgap between LN and PE regions (3.9 and 3.65 eV, respectively), as discussed elsewhere.[4,17,22] More continuous nanostructures are expected to form for longer deposition times, as shown previously.[4] Profiles of the *y*-averaged images recorded after the Ag deposition (Figs. 1(d)–1(f)) are shown as black lines in Figs. 1(g)–1(i), respectively. From Fig. 1(g), Ag can clearly be seen to have deposited both in the LD and RIE regions, however, for larger PE depths. There is deposition on the LD regions only.

The width of the LD, LN, and RIE regions prior to deposition for all of the samples studied have been measured by analyzing line profiles of the images (n = 10), the results of which are shown in Fig. 2(a). The data show that the H^+-Li^+ exchanged layer expands laterally (under the Ti mask during the PE process) at the expense of the LN and that no changes occur to the width of the RIE region. From Eq. (2), the constant of diffusion under the Ti mask in the *x*-direction is determined to be $0.038 \pm 0.001\ \mu m^2/h$. The width of the Ag nanostructures formed during the photodeposition experiments as a function of PE depth are also shown in Fig. 2(a). The analysis illustrates that the width of the deposited Ag nanoparticles coincides with the LD width, demonstrating that the width of the LD regions is the controlling factor in where the Ag deposits. The width of the nanostructures is plotted versus the measured LD width (Fig. 2(b)), and the slope of the linear fit for the 5 largest PE depths is 0.93. The one outlier is the deposition on the shallowest PE-depth sample, which covers the entire PE (LD + RIE) width, and thus is wider than the original RIE width prior to deposition. Interestingly, the average height of the Ag nanostructures (see Fig. 2(b)) tends to decrease as both LD and Ag nanostructure widths increase. The Ag height data have been determined by subtracting data points from *y*-averaged line profiles of the images before deposition from those after deposition, using the pure LN region, on which no deposition is observed, as a reference (n = 10). The same analysis is performed on the RIE region for the 5 largest PE depths, supporting the conclusion that Ag does not deposit there. The Ag height data suggest that the nucleation of Ag nanoparticles on a bare PE-LD surface is more probable than the growth of existing particles. Thus the initially deposited nanostructures can influence subsequent deposition, an observation that merits further investigation.

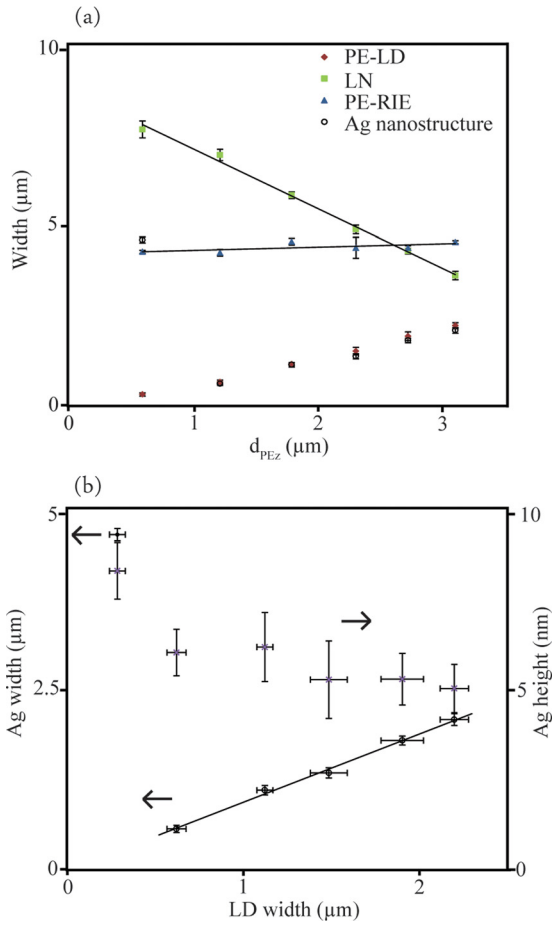

FIG. 2. (a) The lateral diffusion (filled rhombus) and Ag deposition (hollow circle) widths plotted as a function of the PE depth. For reference, the widths of the pure LN region (filled squares) and the RIE portion of the PE region (filled triangles) are also plotted and shown with linear fits for clarity. (b) The Ag nanostructure width (hollow circle) plotted as a function of LD width, showing a linear dependence for the 5 deepest PE depths, and the Ag deposition height (cross) as function of the PE depth.

The observed Ag deposition on the entire PE region for only the shallowest PE depth is an interesting result. First, it demonstrates that RIE damage and incorporation of Cl^- ions alone cannot preclude photoreduction of Ag. Second, it suggests that not only is the PE:LN interface on the crystal surface important in determining where reduction of Ag takes place, but so too is the interface along the *z*-direction, especially when brought in closer proximity to the crystal surface. If we consider the electric field orthogonal to the PE:LN interface along the *z*-axis resulting from the abrupt change in spontaneous polarization, we can envision a case where for shallow PE depths, the photogenerated electrons will migrate towards the surface away from the PE:LN interface. For larger depths, the photogenerated charges may recombine without being subjected to this orthogonal field within the PE region. By varying the PE depth, it should be possible to determine the depth where there is a transition between the two regimes. The transition should also depend on the presence of dopants, e.g., MgO. Similarly, the results suggest that an opposite effect would be observed for

PE-depth studies on the $+z$ crystal surface, i.e., inhibition for shallow depths, and Ag deposition in the RIE region above a certain threshold, however, to fully understand and quantify this effect would require additional studies. We note that photo-oxidation on ferroelectric surfaces can take place,[7] although the full redox reaction is largely ignored when considering photoreduction on ferroelectric surfaces. A limiting factor in the reduction of the silver could be related to the oxidation side of the redox reaction, which would be surface polarity dependent. The recent development of electrochemical strain microscopy[24,25] may help elucidate these processes.

We have demonstrated direct control of the width of silver nanostructures formed via photodeposition on chemically patterned ferroelectric crystals. This has been enabled by varying the depth of the proton exchange process in the lithium niobate crystals, which in turn determines the width of the lateral diffusion region. Our work suggests a route for the fabrication of complex metallic nanostructures on chemically patterned ferroelectric templates. The approach can be implemented in applications in other fields, in particular biosensing, and combined with an exploitation of the underlying PE layers for optical guidance, potentially providing a hybrid optical-ferroelectric-plasmonic platform.

This publication has emanated from research conducted with the financial support of the DGPP and NANOREMEDIES, which are funded under the Programme for Research in Third Level Institutions (PRTLI) Cycle 5 and co-funded by the European Regional Development Fund. We also acknowledge support from the Swedish Research Council (VR 622-2010-526 and 621-2011-4040) and insightful discussions with S. V. Kalinin. The AFM used for this work was funded by Science Foundation Ireland (SFI07/IN1/B031).

[1]G. F. Zheng, F. Patolsky, Y. Cui, W. U. Wang, and C. M. Lieber, Nat. Biotechnol. **23**, 1294 (2005).
[2]M. J. Banholzer, J. E. Millstone, L. Qin, and C. A. Mirkin, Chem. Soc. Rev. **37**, 885 (2008).
[3]P. L. Stiles, J. A. Dieringer, N. C. Shah, and R. R. Van Duyne, Annu. Rev. Anal. Chem. **1**, 601 (2008).
[4]N. C. Carville, M. Manzo, S. Damm, M. Castiella, L. Collins, D. Denning, S. A. L. Weber, K. Gallo, J. H. Rice, and B. J. Rodriguez, ACS Nano **6**, 7373 (2012).
[5]N. C. Carville, M. Manzo, D. Denning, K. Gallo, and B. J. Rodriguez, "Growth mechanism of photoreduced silver nanostructures on periodically proton exchanged lithium niobate: Time and concentration dependence," J. Appl. Phys. (to be published).
[6]J. L. Giocondi and G. S. Rohrer, Chem. Mater. **13**, 241 (2001).
[7]J. L. Giocondi and G. S. Rohrer, J. Phys. Chem. B **105**, 8275 (2001).
[8]S. V. Kalinin, D. A. Bonnell, T. Alvarez, X. Lei, Z. Hu, J. H. Ferris, Q. Zhang, and S. Dunn, Nano Lett. **2**, 589 (2002).
[9]S. V. Kalinin, D. A. Bonnell, T. Alvarez, X. Lei, Z. Hu, R. Shao, and J. H. Ferris, Adv. Mater. **16**, 795–799 (2004).
[10]D. Tiwari and S. Dunn, J. Mater. Sci. **44**, 5063 (2009).
[11]J. N. Hanson, B. J. Rodriguez, R. J. Nemanich, and A. Gruverman, Nanotechnlogy **17**, 4946 (2006).
[12]X. Liu, K. Kitamura, K. Terabe, H. Hatano, and N. Ohashi, Appl. Phys. Lett. **91**, 044101 (2007).
[13]D. Tiwari and S. Dunn, Mater. Lett. **79**, 18 (2012).
[14]A. Haussmann, P. Milde, C. Erler, and L. M. Eng, Nano Lett. **9**, 763 (2009).
[15]Y. Sun and R. J. Nemanich, J. Appl. Phys. **109**, 104302 (2011).
[16]Y. Sun, B. S. Eller, and R. J. Nemanich, J. Appl. Phys. **110**, 084303 (2011).
[17]A. M. Prokhorov and Y. S. Kuz'minov, *Physics and Chemistry of Crystalline Lithium Niobate* (Taylor & Francis, New York, 1990).
[18]M. Manzo, F. Laurell, V. Pasiskevicius, and K. Gallo, Appl. Phys. Lett. **98**, 122910 (2011).
[19]M. Manzo, F. Laurell, V. Pasiskevicius, and K. Gallo, Opt. Mater. Express **1**, 365 (2011).
[20]C. E. Rice and J. L. Jackel, J. Solid State Chem. **41**, 308–314 (1982).
[21]K. S. Chiang, J. Lightwave Technol. **3**, 385 (1985).
[22]D. F. Clark, A. C. G. Nutt, K. K. Wong, P. J. R. Laybourn, and R. M. De la Rue, J. Appl. Phys. **54**, 6218 (1983).
[23]F. Zhou, A. M. Matteo, R. M. De la Rue, and C. N. Ironside, Electron. Lett. **28**, 87 (1992).
[24]A. Kumar, F. Ciucci, A. N. Morozovska, S. V. Kalinin, and S. Jesse, Nat. Chem. **3**, 707 (2011).
[25]A. Kumar, T. M. Arruda, Y. Kim, I. N. Ivanov, S. Jesse, C. W. Bark, N. C. Bristowe, E. Artacho, P. B. Littlewood, C.-B. Eom, and S. V. Kalinin, ACS Nano **6**, 3841–3852 (2012).